

# On the Role of Generalization in Transferability of Adversarial Examples

Yilin Wang\*, Farzan Farnia<sup>†</sup>

## Abstract

Black-box adversarial attacks designing adversarial examples for unseen neural networks (NNs) have received great attention over the past years. While several successful black-box attack schemes have been proposed in the literature, the underlying factors driving the transferability of black-box adversarial examples still lack a thorough understanding. In this paper, we aim to demonstrate the role of the generalization properties of the substitute classifier used for generating adversarial examples in the transferability of the attack scheme to unobserved NN classifiers. To do this, we apply the max-min adversarial example game framework and show the importance of the generalization properties of the substitute NN in the success of the black-box attack scheme in application to different NN classifiers. We prove theoretical generalization bounds on the difference between the attack transferability rates on training and test samples. Our bounds suggest that a substitute NN with better generalization behavior could result in more transferable adversarial examples. In addition, we show that standard operator norm-based regularization methods could improve the transferability of the designed adversarial examples. We support our theoretical results by performing several numerical experiments showing the role of the substitute network’s generalization in generating transferable adversarial examples. Our empirical results indicate the power of Lipschitz regularization methods in improving the transferability of adversarial examples.

## 1 Introduction

Deep neural networks (DNNs) have attained impressive results in many machine learning problems from image recognition [1], speech processing [2], and bioinformatics [3]. The standard evaluation of a trained DNN machine is typically performed over test samples drawn from the same underlying distribution that has generated the empirical training data. The numerous successful applications of deep learning models reported in the literature demonstrate DNNs’ surprising generalization power from training samples to unseen test data. Such promising results on unobserved data despite DNNs’ enormous capacity for memorizing training examples have attracted a lot of attention in the machine learning community.

While DNNs usually achieve satisfactory generalization performance, they have been frequently observed to lack robustness against minor adversarial perturbations to their input data [4, 5, 6], widely known as adversarial attacks. According to these observations, an adversarial attack scheme can generate imperceptible perturbations that fools the DNN classifier to predict wrong labels with high confidence scores. Such adversarial perturbations are usually created through maximizing a target DNN’s prediction loss over a small neighborhood around an input sample. While DNNs often show successful generalization behavior to test samples drawn from the underlying distribution of training data, the minor perturbations designed by adversarial attack schemes can completely undermine their prediction results.

Specifically, adversarial examples have been commonly reported to be capable of transferring to unseen DNN classifiers [7, 8, 9, 10]. Based on these reports, an adversarial example designed for a specific classifier could further alter the prediction of another DNN machine with a different architecture and training set.

---

\*Department of Computer Science and Engineering, The Chinese University of Hong Kong, 1155166083@link.cuhk.edu.hk.

<sup>†</sup>Department of Computer Science and Engineering, The Chinese University of Hong Kong, farnia@cse.cuhk.edu.hk.

Such observations have inspired the development of several *black-box adversarial attack schemes* in which the adversarial examples are designed for a substitute classifier and then are evaluated on a different target DNN.

Several recent papers have attempted to theoretically study the transferability of black-box adversarial attacks. These works have mostly focused on the effects of non-robust features [11, 12, 13] and equilibrium [14, 15] in adversarial training problems on transferable adversarial examples. The mentioned studies reveal the dependency of adversarial examples on non-robust features that can be easily perturbed through minor adversarial noise, and also how the transferability of adversarial examples depend on the equilibrium in the game between the adversary and classifier players. On the other hand, the connections between the generalization behavior of the substitute network and the transferability of the designed examples have not been explored in the literature. Therefore, it remains unclear whether a substitute DNN with better generalization performance can result in more transferable adversarial attacks.

In this work, we attempt to understand the interconnections between the generalization and attack transferability properties of DNNs in black-box adversarial attacks. We aim to show that better generalization performance not only can improve the classification accuracy on unseen data, but further could result in higher transferability rates for the designed adversarial examples. To this end, we analyze the transferability of adversarial examples through the lens of the max-min framework of *adversarial example game* [14]. According to this approach, the adversary player searches for the most transferable attack strategy that reaches the maximum prediction error under the most robust DNN classifier. We focus on the generalization aspect of the adversarial example game, and demonstrate its importance in the transferability power of adversarial perturbations.

Specifically, we focus on the class of norm-bounded adversarial attacks and define the generalization error of a function class’s minimum risk under standard norm-bounded adversarial perturbations. Subsequently, we prove theoretical bounds on the defined generalization metric for multi-layer DNNs with spectrally-normalized weight matrices. Our result extends the operator norm-based generalization bounds [16, 17, 18] in the deep learning literature to the adversarial example game, which enables us to bound the generalization error for the transferability performance of norm-bounded adversarial attack strategies. Also, the shown generalization bound suggests the application of Lipschitz regularization methods in training the substitute DNN in order to improve the transferability of designed adversarial examples.

Finally, we numerically evaluate our theoretical results on multiple standard image recognition datasets and DNN architectures. Our empirical results further support the existing connections between the generalization and transferability properties of black-box adversarial attacks. The numerical findings demonstrate that a better generalization score for the substitute DNN could significantly boost the transferability rate of designed adversarial examples. In addition, we empirically demonstrate that both explicit and implicit regularization techniques can help generating more transferable examples. We validate this result for explicit Lipschitz regularization and implicit early-stopping schemes. We can summarize the main contributions of our work as follows:

- Drawing connections between the generalization properties of the substitute DNN classifier and the transferability rate of designed adversarial examples
- Proving generalization error bounds on the difference between the transferability rates of DNN-based adversarial examples designed for training and test data
- Demonstrating the power of Lipschitz regularization and early stopping methods in generating more transferable adversarial examples
- Conducting numerical experiments on the generalization and transferability aspects of black-box adversarial attacks

## 2 Related Work

Transferability of adversarial examples has been extensively studied in the deep learning literature. The related literature includes a large body of papers [8, 9, 19, 20, 21, 22, 23, 24, 25] proposing black-box adversarial

attack schemes aiming to transfer from a source DNN to an unseen target DNN classifier and several related works [26, 27, 28, 29] on developing robust training mechanisms against black-box adversarial attacks. Also, several game theoretic frameworks have been proposed to analyze the transferability of adversarial examples. The related works [14, 15] study the adversarial example game between the classifier and adversary players. However, these works mostly focus on the equilibrium and convergence behavior in adversarial example games and do not discuss the generalization aspect of the game. In another related work, [30] studies the adversarial learning task through the lens of game theory. Unlike our work, the generalization analysis in [30] focuses only on the generalization behavior of the robust classification rule and not on the generalization properties of the transferable adversary player.

Furthermore, the generalization properties of adversarially-learned models have been the topic of several related papers. References [31, 32] discuss numerical and theoretical results that generalization of adversarially-trained neural nets is inferior to that of standard ERM-learned models with the same number of training data. The related work [33] empirically studies the overfitting phenomenon in adversarial training problems and reveals the different generalization properties of standard and adversarial training schemes. In another study, [34] shows the connection between the generalization of adversarially-learned models and the flatness of weight loss landscape. [35, 36] develop Rademacher-complexity-based generalization bounds for adversarially-trained models which suggest the application of norm-based regularization techniques for improving the generalization behavior of adversarial training methods. [37] proves Pac-Bayes generalization bounds for adversarially-learned DNNs with bounded spectral norms for their weight matrices. Also, [38] performs VC-based generalization analysis for adversarial training schemes and derives upper-bounds on their sample complexity. However, we note that all these papers focus on the generalization of adversarially-trained models and do not study the connection between generalization and transferability of black-box attacks.

### 3 Preliminaries: Adversarial Attacks and Training

In this section, we give a brief review of standard norm-bounded adversarial attack and training schemes. Consider a supervised learning problem where the learner seeks a prediction rule  $f$  from function space  $\mathcal{F}$  to predict a label variable  $Y \in \mathcal{Y}$  from the observation of a  $d$ -dimensional feature vector  $\mathbf{X} \in \mathcal{X}$ . In this work, we focus on the following set of  $L$ -layer neural network functions with activation function  $\phi$ :

$$\mathcal{F}_{\mathcal{W}} = \left\{ f_{\mathbf{w}} : f_{\mathbf{w}}(\mathbf{x}) = W_L \phi(W_{L-1} \phi(\dots W_1 \phi(W_0 \mathbf{x})), \mathbf{w} \in \mathcal{W} \right\}. \quad (1)$$

In the above, we use vector  $\mathbf{w}$  belonging to feasible set  $\mathcal{W}$  to parameterize the  $L$ -layer neural net  $f_{\mathbf{w}}$ . According to this notation,  $\mathbf{w}$  concatenates all the entries of the neural net's weight matrices  $W_0, \dots, W_L$ .

Given a loss function  $\ell$  and  $n$  training samples in dataset  $S = \{(\mathbf{x}_i, y_i)_{i=1}^n\}$ , the standard risk minimization approach aims to find the prediction rule  $f^* \in \mathcal{F}_{\mathcal{W}}$  minimizing the expected loss (risk)  $\mathbb{E}[\ell(f(\mathbf{X}), Y)]$  where the expectation is taken according to the underlying distribution of data  $P_{\mathbf{X}, Y}$ . Since the supervised learner only observes the training samples and lacks any further knowledge of the underlying  $P_{\mathbf{X}, Y}$ , the empirical risk minimization (ERM) framework sets out to minimize the empirical risk function estimated using the training examples:

$$\min_{\mathbf{w} \in \mathcal{W}} \frac{1}{n} \sum_{i=1}^n \ell(f_{\mathbf{w}}(\mathbf{x}_i), y_i). \quad (2)$$

However, the ERM learner typically lacks robustness to norm-bounded adversarial perturbations. A standard approach to generate a norm-bounded adversarial perturbation is through maximizing the loss function over a norm ball around a given data point  $(\mathbf{x}, y)$ :

$$\max_{\boldsymbol{\delta}: \|\boldsymbol{\delta}\| \leq \epsilon} \ell(f(\mathbf{x} + \boldsymbol{\delta}), y). \quad (3)$$

Here  $\boldsymbol{\delta} \in \mathbb{R}^d$  represents the  $d$ -dimensional perturbation vector added to the feature vector  $\mathbf{x}$ , and  $\|\cdot\|$  denotes a norm function used to measure the attack power that is bounded by parameter  $\epsilon \geq 0$ .

In order to gain robustness against norm-bounded perturbations, the adversarial training (AT) scheme [39] alters the ERM objective function to the expected worst-case loss function over norm-bounded adversarial perturbations and solves the following min-max optimization problem:

$$\min_{\mathbf{w} \in \mathcal{W}} \frac{1}{n} \sum_{i=1}^n \left[ \max_{\delta_i: \|\delta_i\| \leq \epsilon} \ell(f_{\mathbf{w}}(\mathbf{x}_i + \delta_i), y_i) \right] \equiv \min_{\mathbf{w} \in \mathcal{W}} \max_{\substack{\delta_1, \dots, \delta_n: \\ \forall i, \|\delta_i\| \leq \epsilon}} \frac{1}{n} \sum_{i=1}^n [\ell(f_{\mathbf{w}}(\mathbf{x}_i + \delta_i), y_i)] \quad (4)$$

Note that the above minimax problem indeed estimates the solution to the following learning problem formulated over the true distribution of data  $P_{\mathbf{X}, Y}$ :

$$\min_{\mathbf{w} \in \mathcal{W}} \mathbb{E}_{(\mathbf{X}, Y) \sim P} \left[ \max_{\delta: \|\delta\| \leq \epsilon} \ell(f_{\mathbf{w}}(\mathbf{X} + \delta), Y) \right]. \quad (5)$$

It can be seen that the above optimization problem is indeed equivalent to the following min-max problem where the maximization is performed over  $\Delta_\epsilon$  containing all mappings  $\delta: \mathcal{X} \times \mathcal{Y} \rightarrow \mathbb{R}^d$  whose output is  $\epsilon$ -norm-bounded, i.e.  $\forall \mathbf{x}, y: \|\delta(\mathbf{x}, y)\| \leq \epsilon$ :

$$\min_{\mathbf{w} \in \mathcal{W}} \max_{\delta \in \Delta_\epsilon} \mathbb{E}_{\mathbf{X}, Y \sim P} [\ell(f_{\mathbf{w}}(\mathbf{X} + \delta(\mathbf{X}, Y)), Y)]. \quad (6)$$

In next sections, we will discuss the association between the above min-max problem and the adversarial example game for generating transferable adversarial examples.

## 4 A Max-Min Approach to Transferable Adversarial Examples

Transferability of adversarial examples has been extensively studied in the literature. A useful framework to theoretically study transferable examples is the max-min framework of *adversarial example game (AEG)* [14]. According to this approach, the adversary searches for the most transferable attack scheme  $\delta \in \Delta$  from a set of attack strategies  $\Delta$  that achieves the maximum expected loss under the most robust classifier  $f_{\mathbf{w}} \in \mathcal{F}_{\mathcal{W}}$  from DNN function space  $\mathcal{F}_{\mathcal{W}}$ . Therefore, the AEG approach reduces the transferable adversary’s task to solving the following max-min optimization problem:

$$\max_{\delta \in \Delta} \min_{\mathbf{w} \in \mathcal{W}} \frac{1}{n} \sum_{i=1}^n \left[ \ell(f_{\mathbf{w}}(\mathbf{x}_i + \delta(\mathbf{x}_i, y_i)), y_i) \right] \quad (7)$$

The above bi-level optimization problem indeed swaps the maximization and minimization order of the AT optimization problem, and focuses on the max-min version of the min-max AT optimization task. Note that as shown in [15], the adversarial example game is in general not guaranteed to possess a pure Nash equilibrium where each player’s deterministic strategy is optimal when fixing the other player’s strategy. As a result of the lack of pure Nash equilibria, the AEG max-min and AT min-max optimization problems may not share any common solutions.

Note that the AEG framework introduces the following metric for evaluating the transferability of an attack scheme  $\delta: \mathcal{X} \times \mathcal{Y} \rightarrow \mathbb{R}^d$ :

$$\widehat{\mathcal{L}}_{\text{transfer}}(\delta) := \min_{\mathbf{w} \in \mathcal{W}} \frac{1}{n} \sum_{i=1}^n [\ell(f_{\mathbf{w}}(\mathbf{x}_i + \delta(\mathbf{x}_i, y_i)), y_i)] \quad (8)$$

The above transferability score indeed estimates the following score measuring transferability under the underlying distribution  $P_{\mathbf{X}, Y}$ :

$$\mathcal{L}_{\text{transfer}}(\delta) := \min_{\mathbf{w} \in \mathcal{W}} \mathbb{E}_{(\mathbf{X}, Y) \sim P} \left[ \ell(f_{\mathbf{w}}(\mathbf{X} + \delta(\mathbf{X}, Y)), Y) \right]. \quad (9)$$

Based on this discussion, the AEG optimization problem in (7) similarly estimates the solution to the following max-min AEG problem formed around the underlying distribution  $P_{\mathbf{X}, Y}$ :

$$\max_{\delta \in \Delta} \mathcal{L}_{\text{transfer}}(\delta) \equiv \max_{\delta \in \Delta} \min_{\mathbf{w} \in \mathcal{W}} \mathbb{E}_{(\mathbf{X}, Y) \sim P} \left[ \ell(f_{\mathbf{w}}(\mathbf{X} + \delta(\mathbf{X}, Y)), Y) \right]. \quad (10)$$

Therefore, the primary goal of the transferable adversary is to solve the above problem targeting the distribution of test data instead of training examples. However, since the true distribution is unknown to the adversary, the AEG framework switches to the empirical max-min problem (7). This discussion motivates the following definition of the generalization error for adversarial examples' transferability performance:

**Definition 1.** We define the generalization error of an attack scheme  $\delta : \mathcal{X} \times \mathcal{Y} \rightarrow \mathbb{R}^d$  over DNN classifier space  $\mathcal{F}_{\mathcal{W}}$  as follows:

$$\begin{aligned} \epsilon_{\text{gen}}(\delta) &:= \widehat{\mathcal{L}}_{\text{transfer}}(\delta) - \mathcal{L}_{\text{transfer}}(\delta) \\ &= \min_{\mathbf{w} \in \mathcal{W}} \left\{ \frac{1}{n} \sum_{i=1}^n \left[ \ell(f_{\mathbf{w}}(\mathbf{x}_i + \delta(\mathbf{x}_i, y_i)), y_i) \right] \right\} - \min_{\mathbf{w} \in \mathcal{W}} \left\{ \mathbb{E} \left[ \ell(f_{\mathbf{w}}(\mathbf{X} + \delta(\mathbf{X}, Y)), Y) \right] \right\}. \end{aligned} \quad (11)$$

In order for a black-box adversarial attack to be effective, we need the attack scheme to generalize well from training samples to test data, and based on the max-min AEG framework the generalization error is defined in the specific sense of Definition 1. In next sections, we study how the choice of substitute DNN will affect the above generalization error of the resulting adversarial attack scheme.

## 5 A Generalization Error Bound for Adversarial Example Games

In this section, we aim to analyze the generalization error of a black-box adversarial attack scheme based on the substitute classifier of a  $L$ -layer DNN  $\mathcal{H}_{\mathcal{W}}$ . To characterize a one-to-one correspondence between the choice of the DNN weights and the assigned attack scheme, we consider the following definition of an optimal attack scheme for a substitute neural net  $h_{\mathbf{w}} \in \mathcal{H}_{\mathcal{W}}$ .

**Definition 2.** Given a classifier  $h_{\mathbf{w}}$ , we call the attack scheme  $\delta_{\mathbf{w}}^* : \mathcal{X} \times \mathcal{Y} \rightarrow \mathbb{R}^d$   $\lambda$ -optimal if it solves the following optimization problem:

$$\max_{\delta : \mathcal{X} \times \mathcal{Y} \rightarrow \mathbb{R}^d} \mathbb{E}[\ell(h_{\mathbf{w}}(\mathbf{X} + \delta(\mathbf{X}, Y)), Y)] - \frac{\lambda}{2} \mathbb{E}[\|\delta(\mathbf{X}, Y)\|^2].$$

Note that the above definition of optimal attack scheme employs a regularization term to penalize the averaged norm-squared of designed perturbations. As shown in the next proposition, this definition results in a one-to-one correspondence between  $\lambda$ -optimal attack schemes and  $\lambda$ -smooth DNN classifiers. We defer the proof of the theoretical results to the Appendix.

**Proposition 1.** Consider the  $L_2$ -norm function  $\|\cdot\|_2$  for measuring the attack power. Suppose that the composition  $\ell \circ h_{\mathbf{w}}$  is a  $\lambda$ -smooth differentiable function of  $\mathbf{x}$ , i.e. for every  $\mathbf{x}, \mathbf{x}', y$  we have  $\|\nabla_{\mathbf{x}} \ell(h_{\mathbf{w}}(\mathbf{x}), y) - \nabla_{\mathbf{x}} \ell(h_{\mathbf{w}}(\mathbf{x}'), y)\|_2 \leq \lambda \|\mathbf{x} - \mathbf{x}'\|_2$ . Then, there exists a unique  $\lambda$ -optimal attack scheme  $\delta^*(\mathbf{x}, y)$  for  $h_{\mathbf{w}}$  given by:

$$\delta^*(\mathbf{x}, y) = \left( \text{Id}_{\mathbf{x}} - \frac{1}{\lambda} \nabla_{\mathbf{x}} \ell \circ h_{\mathbf{w}} \right)^{-1} (\mathbf{x}, y) - \mathbf{x}.$$

In the above equation  $\text{Id}_{\mathbf{x}}$  represents the identity function on feature vector  $\mathbf{x}$ , and  $(\cdot)^{-1}$  denotes the inverse of an invertible transformation.

The above proposition reveals a bijection between smooth DNN classifiers and optimal attack schemes. Therefore, in our generalization analysis, we focus on bounding the generalization error for the resulting  $\lambda$ -optimal attack schemes corresponding to  $\lambda$ -smooth DNN substitute classifiers.

In the following theorem, we show a generalization error bound for the class of  $\lambda$ -optimal black-box attack schemes coming from spectrally-regularized DNN functions. We note that our proof of the theorem extends the generalization analysis of spectrally-normalized neural networks in [16] to the adversarial settings which is different from the existing Rademacher complexity-based and Pac-Bayes-based generalization analyses in the related works [35, 36, 37] on generalization of adversarial training methods. In the theorem, we use the following set of assumptions on the loss function  $\ell$  and the target and substitute classes of neural networks. Also, note that  $\|\cdot\|_2$  denotes the  $L_2$ -operator (spectral) norm in application to a matrix, i.e. the matrix's maximum singular value, and  $\|\cdot\|_{2,1}$  denotes the  $(2,1)$ -norm of a matrix which is the summation of the  $L_2$ -norms of the matrix's rows.

**Assumption 1.** *Loss function  $\ell(y, y')$  is a  $c$ -bounded, 1-Lipschitz, and 1-smooth function of the input  $y$ , i.e. for every  $y_1, y_2, y' \in \mathcal{Y}$  we have  $|\ell(y_1, y')| \leq c$ ,  $|\ell(y_1, y') - \ell(y_2, y')| \leq \|y_1 - y_2\|_2$ , and  $\|\nabla_y \ell(y_1, y') - \nabla_y \ell(y_2, y')\|_2 \leq \|y_1 - y_2\|_2$ .*

**Assumption 2.** *The set of substitute DNNs in the black-box attack scheme  $\mathcal{H}_{\mathcal{W}} = \{h_{\mathbf{w}} : \mathbf{w} \in \mathcal{W}\}$  contains  $L$ -layer neural networks  $h_{\mathbf{w}}(\mathbf{x}) = W_L \phi_L(W_{L-1} \phi_{L-1}(\cdots W_1 \phi_1(W_0 \mathbf{x}))$ . We suppose that the dimensions of matrices  $W_0, \dots, W_k$  is bounded by  $D$ , and assume every activation  $\phi_i$  satisfies  $\phi_i(0) = 0$  and is  $\gamma_i$ -Lipschitz and  $\gamma_i$ -smooth, i.e.  $\max\{|\phi_i'(z)|, |\phi_i''(z)|\} \leq \gamma_i$  holds for every  $z \in \mathbb{R}$ .*

**Assumption 3.** *The class of target classifiers  $\mathcal{F}_{\mathcal{V}} = \{f_{\mathbf{v}} : \mathbf{v} \in \mathcal{V}\}$  consists of  $K$ -layer neural network functions  $f_{\mathbf{v}}(\mathbf{x}) = V_K \psi_L(V_{L-1} \psi_{L-1}(\cdots V_1 \psi_1(V_0 \mathbf{x}))$  with activation function  $\psi_i$ 's. We suppose that the dimensions of matrices  $V_0, \dots, V_k$  is bounded by  $D$ . Also, we assume every  $\psi_i$  satisfies  $\psi_i(0) = 0$  and is  $\xi_i$ -Lipschitz, i.e.  $\max_z |\psi_i'(z)| \leq \xi_i$ . Also, we define the capacity  $R_{\mathcal{V}}$  as*

$$R_{\mathcal{V}} := \sup_{\mathbf{v} \in \mathcal{V}} \left\{ \left( \prod_{i=0}^K \xi_i \|V_i\|_2 \right) \left( \sum_{i=0}^K \frac{\|V_i^\top\|_{2,1}^{2/3}}{\|V_i\|_2^{2/3}} \right)^{3/2} \right\}.$$

**Theorem 1.** *Suppose that the loss function, substitute DNN, and target DNN in a black-box adversarial attack satisfy Assumptions 1, 2 and 3. Assuming  $\|\mathbf{X}\|_2 \leq B$  for the  $n \times d$  data matrix  $\mathbf{X}$  and  $\lambda(1 - \tau) \geq (\prod_{i=0}^L \gamma_i \|W_i\|_2) \sum_{i=0}^L \prod_{j=0}^L \gamma_j \|W_j\|_2$  holds for constant  $\tau > 0$  and every  $\mathbf{w} \in \mathcal{W}$ , then for every  $\omega > 0$  with probability at least  $1 - \omega$  the following bound will hold for every  $\mathbf{w} \in \mathcal{W}$ :*

$$\epsilon_{\text{gen}}(\delta_{\mathbf{w}}^*) \leq \mathcal{O} \left( c \sqrt{\frac{\log(1/\omega)}{n}} + \frac{(B + \frac{L_{\mathbf{w}}}{\lambda})(R_{\mathcal{V}} + \frac{1}{\tau^2} L_{\mathbf{w}} R_{\mathbf{w}}) \log(n)}{n} \log(D) \right) \quad (12)$$

where the Lipschitz and capacity terms  $L_{\mathbf{w}}, R_{\mathbf{w}}$  are defined as:

$$L_{\mathbf{w}} := \prod_{i=0}^L \gamma_i \|W_i\|_2, \quad R_{\mathbf{w}} := \left( \sum_{i=0}^L \prod_{j=0}^i \gamma_j \|W_j\|_2 \right) \left( \sum_{i=0}^L \frac{\|W_i^\top\|_{2,1}^{2/3}}{\|W_i\|_2^{2/3}} \right)^{3/2}. \quad (13)$$

The above theorem bounds the generalization error of the attack scheme  $\delta_{\mathbf{w}}^*$  corresponding to the substitute DNN  $f_{\mathbf{w}}$  in terms of the spectral capacity of the substitute network. As a result, this bound motivates norm-based spectral regularization [40, 41, 37] for improving the generalization performance of black-box attack schemes.

## 6 Numerical Results

In this section, we provide the results of our numerical experiments for validating the connection between the generalization and transferability properties of black-box adversarial attacks. The numerical discussion focuses on the question of whether achieving a better generalization score for the substitute DNN can improve the success of the designed perturbations in application to a different DNN classifier. To answer this question,

we tested an explicit norm-based regularization method, spectral normalization [40, 37], as well as an implicit regularization technique, early stopping [42, 33], to evaluate the power of these regularization methods in attaining more transferable black-box attacks.

For generating norm-bounded perturbations, we used standard projected gradient descent (PGD) and fast gradient method (FGM) [43] to design perturbations. We implemented the PGD and FGM algorithms by projecting the perturbations according to both standard  $L_2$ -norm and  $L_\infty$ -norm, where the latter results in the widely-used fast gradient sign method (FGSM) attack scheme [43] in the FGM case. For simulating  $L_2$ -norm-bounded perturbations, we chose the maximum  $L_2$ -norm (attack power) as  $\epsilon = \gamma \mathbb{E}_{\hat{P}}[\|X\|_2]$  with  $\gamma = 0.05$  unless stated otherwise. For  $L_\infty$ -norm-bounded attacks, we chose  $\epsilon = 8/255$  for the normalized samples. For optimizing PGD perturbations, we applied  $r = 15$  PGD steps, where we used the standard rule  $\alpha = 1.5\epsilon/r$  to choose the stepsize parameter  $\alpha$ . We trained every DNN model for 100 epochs using the Adam optimizer [44] with a batch-size of 128. The numerical experiments were implemented using the PyTorch [45] platform and were run on one standard RTX-3090 GPU.

In our experiments, we used three standard image recognition datasets: 1) CIFAR-10 [46], 2) CIFAR-100 [46], 3) SVHN [47], and the following four neural network architectures: 1) AlexNet [48], 2) Inception-Net [49], 3) VGG-16 [50], 4) ResNet-18 [51]. In the reported results, we evaluate a prediction model’s generalization performance using the accuracy gap between the training and test sets. For evaluating the transferability performance, we used the generated black-box adversarial examples and measured the transferability rate as the target network’s averaged classification error over the designed adversarial examples on the test set. Therefore, a higher transferability rate implies more transferable adversarial examples.

In the numerical evaluation of the adversarial examples’ transferability to the target models, we only considered those samples whose original unperturbed versions had been labeled correctly by the target DNN, as we expect the clean version of an adversarial example for the target DNN to be at least labeled correctly by this classifier. In addition, we used different training sets for the substitute and target classifiers to separate the generalization effects of the substitute and target DNNs. To do this, we split the training set in half and used each half for training one of the two classifiers. Finally, in consistence with our theoretical analysis, we used PGD adversarial training for training the substitute DNN model and applied standard ERM training for training the target DNNs.

## 6.1 Transferability and Generalization under Spectral Regularization

We evaluated the generalization and transefrability performance of the discussed black-box attack schemes for Lipschitz-regularized neural nets. To apply spectral regularization, we used the spectral normalization method [41, 37] constraining the  $L_2$ -operator norm of the substitute DNN’s weight matrices. We define hyper-parameter  $\beta$  as the maximum allowed  $L_2$ -operator norm. Then, the standard spectral normalization method modifies each weight matrix  $W_i$  in (1) to the following  $\widetilde{W}_i$ :

$$\widetilde{W}_i := \frac{W_i}{\max\{1, \frac{\|W_i\|_2}{\beta}\}} = \begin{cases} W_i & \text{if } \|W_i\|_2 \leq \beta, \\ \frac{\beta}{\|W_i\|_2} W_i & \text{otherwise.} \end{cases} \quad (14)$$

The above operation will regularize the matrix’s operator norm to be upper-bounded by  $\beta$ .

Figure 1 shows the generalization error of the model and attack transferability rates of the generated perturbations using the substitute classifier AlexNet and Inception-Net under different spectral-norm hyper-parameter  $\beta$ ’s. The numerical results show that in all cases through applying the stronger regularization coefficients  $\beta = 1.0, 1.3$ , the AlexNet and Inception classifiers achieve the highest generalization performance and attack transferability rates to the target ResNet-18 and VGG-16. Therefore, spectral regularization not only helped the DNN classifier attain better generalization score, which is an expected outcome, but further improved the transferability of the designed perturbations to unseen DNNs with different architectures. These numerical results suggest the impact of the substitute network’s generalization error on the success of the adversarial examples on other DNNs.

Table 1 shows our numerical results validating the connection between the substitute DNN’s generalization and  $L_2$ -norm-based designed adversarial examples’ transferability. In this table, we report the performance of spectral regularization under the best  $\beta$  hyperparameter for validation samples. As can be seen in this

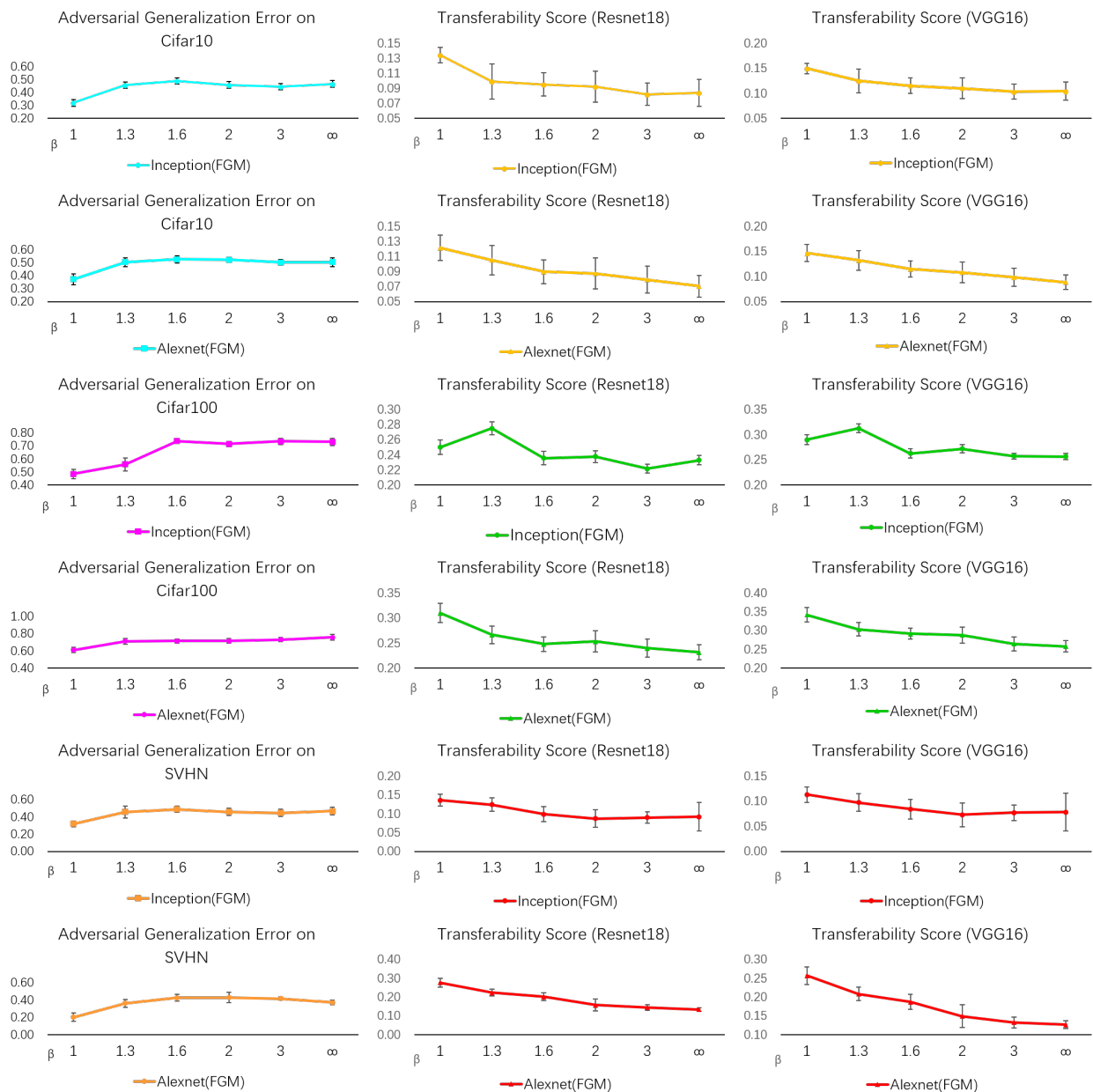


Figure 1: Generalization errors of substitute DNNs (the lower the better), and transferability rates of adversarial examples generated from the substitute model (the higher the better) for CIFAR-10 (rows 1-2), CIFAR-100 (rows 3-4) and SVHN (rows 5-6) datasets. ResNet18 and VGG-16 architectures were used as the target DNNs.



Table 1: Generalization error (Gen. Err.) and  $L_2$ -norm-based adversarial examples’ transferability rates on three image datasets, with and without spectral regularization ( $\beta = \infty$  means no spectral regularization).

Dataset	Model	Method	$\beta$	Gen.Err.	Transferability Rate(VGG16)	Transferability Rate(ResNet18)
Cifar10	AlexNet	PGD	$\infty$	0.545	0.105	0.087
			1.0	0.342	0.162	0.139
		FGM	$\infty$	0.505	0.089	0.070
			1.0	0.451	0.147	0.122
	Inception	PGD	$\infty$	0.508	0.104	0.084
			1.0	0.258	0.150	0.134
FGM	$\infty$	0.466	0.092	0.078		
	1.0	0.320	0.136	0.113		
Cifar100	AlexNet	PGD	$\infty$	0.789	0.229	0.260
			1.0	0.601	0.323	0.353
		FGM	$\infty$	0.758	0.258	0.232
			1.0	0.611	0.342	0.310
	Inception	PGD	$\infty$	0.602	0.303	0.270
			1.3	0.494	0.330	0.301
FGM	$\infty$	0.717	0.268	0.236		
	1.3	0.558	0.313	0.275		
SVHN	AlexNet	PGD	$\infty$	0.298	0.211	0.225
			1.0	0.199	0.276	0.292
		FGM	$\infty$	0.373	0.134	0.126
			1.0	0.203	0.277	0.257
	Inception	PGD	$\infty$	0.342	0.193	0.177
			1.0	0.115	0.339	0.313
FGM	$\infty$	0.373	0.134	0.126		
	1.0	0.203	0.277	0.257		

Table 2: Generalization error (Gen. Err.) and adversarial examples’ transferability rates on three image datasets, with and without early stopping (ES)

Dataset	Model	Method	Gen. Err.	Transferability Rate(VGG16)	Transferability Rate(ResNet18)
Cifar10	Inception	PGD	0.517	0.127	0.104
		PGD-ES	0.073	0.198	0.172
		FGM	0.467	0.100	0.089
		FGM-ES	0.126	0.170	0.147
	AlexNet	PGD	0.579	0.098	0.077
		PGD-ES	0.061	0.154	0.136
		FGM	0.520	0.100	0.087
		FGM-ES	0.092	0.152	0.127
SVHN	Inception	PGD	0.341	0.207	0.220
		PGD-ES	0.057	0.298	0.322
		FGM	0.380	0.136	0.129
		FGM-ES	0.180	0.213	0.219
	AlexNet	PGD	0.307	0.211	0.228
		PGD-ES	0.030	0.256	0.278
		FGM	0.373	0.157	0.170
		FGM-ES	0.064	0.241	0.260

table, spectral regularization manages to consistently improve the transferability rates of the adversarial examples, which confirms our hypothesis that better generalization will lead to more transferable adversarial examples. Due to the 9-page space limit, we defer the presentation of our numerical results for  $L_\infty$ -norm-based adversarial examples to the Appendix.

## 6.2 Transferability and Generalization under Early Stopping

Next, we used the implicit regularization mechanism of early stopping [42] to validate that better generalization achieved under early stopping can help generating more transferable adversarial examples. To perform early stopping, we used 30% of the original test set as the validation set, and used the remaining 70% to measure the test accuracy. We stopped the DNN training when the trained model achieved its best performance on the validation samples. Due to the 9-page space limit, here we present the CIFAR-10 and SVHN numerical results in Table 2. The complete set of obtained numerical results is deferred to the Appendix. Again, our numerical results suggest that both the generalization and transferability scores considerably improve under the early stopping regularization. The observation is consistent with our hypothesis on the impact of the generalization behavior of the substitute network on the transferability of adversarial examples.

Finally, Figure 2 illustrates 12 uniformly-sampled transferable adversarial examples under spectral regularization and early stopping. We note that the adversarial examples designed by the unregularized DNN for these test samples failed to transfer to the target DNNs. We also observed that the transferable perturbations generated from a regularized DNN had sharper edges and less noise power in the background, and concentrated the perturbation’s power on the central part of the image.

## 7 Conclusion

In this paper, we provided theoretical and numerical evidence on how the generalization properties of a substitute neural network can influence the transferability of the generated adversarial examples to other classifiers. While the transferability of black-box adversarial attacks and generalization power of the substitute classifier may seem two orthogonal factors, our results indicate existing interconnections between the two aspects. We note that our work develops standard uniform-convergence generalization bounds, and an interesting future direction is to apply the recently-developed generalization analysis of

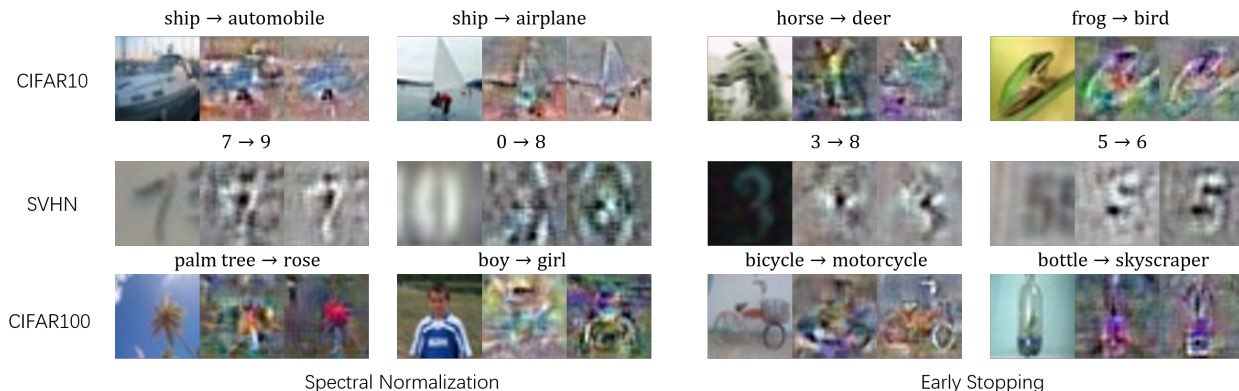


Figure 2: Visualization of adversarial perturbations. Each set of three pictures shows the original sample, the untransferable perturbation from the unregularized DNN, and the transferable perturbation generated by the regularized model (left to right).  $A \rightarrow B$  indicates the groundtruth label  $A$  and the transferable example’s predicted label  $B$ .

overparameterized function spaces to gain a better understanding of the role of benign overfitting in the transferability of adversarial examples. Also, our experimental results motivate further studies of how other popular regularization methods in deep learning, such as batch normalization and dropout, can affect the transferability of designed adversarial examples.

## References

- [1] Alex Krizhevsky, Geoffrey Hinton, et al. Learning multiple layers of features from tiny images. 2009.
- [2] Li Deng, Jinyu Li, Jui-Ting Huang, Kaisheng Yao, Dong Yu, Frank Seide, Michael Seltzer, Geoff Zweig, Xiaodong He, Jason Williams, et al. Recent advances in deep learning for speech research at microsoft. In *2013 IEEE international conference on acoustics, speech and signal processing*, pages 8604–8608. IEEE, 2013.
- [3] Babak Alipanahi, Andrew Delong, Matthew T Weirauch, and Brendan J Frey. Predicting the sequence specificities of dna-and rna-binding proteins by deep learning. *Nature biotechnology*, 33(8):831–838, 2015.
- [4] Christian Szegedy, Wojciech Zaremba, Ilya Sutskever, Joan Bruna, Dumitru Erhan, Ian Goodfellow, and Rob Fergus. Intriguing properties of neural networks. *arXiv preprint arXiv:1312.6199*, 2013.
- [5] Battista Biggio, Iginio Corona, Davide Maiorca, Blaine Nelson, Nedim Šrndić, Pavel Laskov, Giorgio Giacinto, and Fabio Roli. Evasion attacks against machine learning at test time. In *Joint European conference on machine learning and knowledge discovery in databases*, pages 387–402. Springer, 2013.
- [6] Ian J Goodfellow, Jonathon Shlens, and Christian Szegedy. Explaining and harnessing adversarial examples. *arXiv preprint arXiv:1412.6572*, 2014.
- [7] Florian Tramèr, Alexey Kurakin, Nicolas Papernot, Ian Goodfellow, Dan Boneh, and Patrick McDaniel. Ensemble adversarial training: Attacks and defenses. *arXiv preprint arXiv:1705.07204*, 2017.
- [8] Andrew Ilyas, Logan Engstrom, Anish Athalye, and Jessy Lin. Black-box adversarial attacks with limited queries and information. In *International Conference on Machine Learning*, pages 2137–2146. PMLR, 2018.
- [9] Minhao Cheng, Thong Le, Pin-Yu Chen, Jinfeng Yi, Huan Zhang, and Cho-Jui Hsieh. Query-efficient hard-label black-box attack: An optimization-based approach. *arXiv preprint arXiv:1807.04457*, 2018.

- [10] Wen Zhou, Xin Hou, Yongjun Chen, Mengyun Tang, Xiangqi Huang, Xiang Gan, and Yong Yang. Transferable adversarial perturbations. In *Proceedings of the European Conference on Computer Vision (ECCV)*, pages 452–467, 2018.
- [11] Florian Tramèr, Nicolas Papernot, Ian Goodfellow, Dan Boneh, and Patrick McDaniel. The space of transferable adversarial examples. *arXiv preprint arXiv:1704.03453*, 2017.
- [12] Andrew Ilyas, Shibani Santurkar, Dimitris Tsipras, Logan Engstrom, Brandon Tran, and Aleksander Madry. Adversarial examples are not bugs, they are features. *Advances in neural information processing systems*, 32, 2019.
- [13] Nathan Inkawhich, Wei Wen, Hai Helen Li, and Yiran Chen. Feature space perturbations yield more transferable adversarial examples. In *Proceedings of the IEEE/CVF Conference on Computer Vision and Pattern Recognition*, pages 7066–7074, 2019.
- [14] Joey Bose, Gauthier Gidel, Hugo Berard, Andre Cianflone, Pascal Vincent, Simon Lacoste-Julien, and Will Hamilton. Adversarial example games. *Advances in neural information processing systems*, 33:8921–8934, 2020.
- [15] Laurent Meunier, Meyer Scetbon, Rafael B Pinot, Jamal Atif, and Yann Chevaleyre. Mixed nash equilibria in the adversarial examples game. In *International Conference on Machine Learning*, pages 7677–7687. PMLR, 2021.
- [16] Peter L Bartlett, Dylan J Foster, and Matus J Telgarsky. Spectrally-normalized margin bounds for neural networks. In *Advances in Neural Information Processing Systems*, pages 6240–6249, 2017.
- [17] Behnam Neyshabur, Srinadh Bhojanapalli, and Nathan Srebro. A pac-bayesian approach to spectrally-normalized margin bounds for neural networks. *arXiv preprint arXiv:1707.09564*, 2017.
- [18] Colin Wei and Tengyu Ma. Improved sample complexities for deep networks and robust classification via an all-layer margin. *arXiv preprint arXiv:1910.04284*, 2019.
- [19] Arjun Nitin Bhagoji, Warren He, Bo Li, and Dawn Song. Practical black-box attacks on deep neural networks using efficient query mechanisms. In *Proceedings of the European Conference on Computer Vision (ECCV)*, pages 154–169, 2018.
- [20] Moustafa Alzantot, Yash Sharma, Supriyo Chakraborty, Huan Zhang, Cho-Jui Hsieh, and Mani B Srivastava. Genattack: Practical black-box attacks with gradient-free optimization. In *Proceedings of the Genetic and Evolutionary Computation Conference*, pages 1111–1119, 2019.
- [21] Shuyu Cheng, Yinpeng Dong, Tianyu Pang, Hang Su, and Jun Zhu. Improving black-box adversarial attacks with a transfer-based prior. *Advances in neural information processing systems*, 32, 2019.
- [22] Seungyong Moon, Gaon An, and Hyun Oh Song. Parsimonious black-box adversarial attacks via efficient combinatorial optimization. In *International Conference on Machine Learning*, pages 4636–4645. PMLR, 2019.
- [23] Chuan Guo, Jacob Gardner, Yurong You, Andrew Gordon Wilson, and Kilian Weinberger. Simple black-box adversarial attacks. In *International Conference on Machine Learning*, pages 2484–2493. PMLR, 2019.
- [24] Hadi Mohaghegh Dolatabadi, Sarah Erfani, and Christopher Leckie. Advflow: Inconspicuous black-box adversarial attacks using normalizing flows. *Advances in Neural Information Processing Systems*, 33:15871–15884, 2020.
- [25] Run Wang, Felix Juefei-Xu, Qing Guo, Yihao Huang, Xiaofei Xie, Lei Ma, and Yang Liu. Amora: Black-box adversarial morphing attack. In *Proceedings of the 28th ACM International Conference on Multimedia*, pages 1376–1385, 2020.

- [26] Alexander Levine and Soheil Feizi. Robustness certificates for sparse adversarial attacks by randomized ablation. In *Proceedings of the AAAI Conference on Artificial Intelligence*, volume 34, pages 4585–4593, 2020.
- [27] Hadi Salman, Mingjie Sun, Greg Yang, Ashish Kapoor, and J Zico Kolter. Denoised smoothing: A provable defense for pretrained classifiers. *Advances in Neural Information Processing Systems*, 33:21945–21957, 2020.
- [28] Sahil Singla and Soheil Feizi. Second-order provable defenses against adversarial attacks. In *International conference on machine learning*, pages 8981–8991. PMLR, 2020.
- [29] Huiying Li, Shawn Shan, Emily Wenger, Jiayun Zhang, Haitao Zheng, and Ben Y Zhao. Blacklight: Defending black-box adversarial attacks on deep neural networks. *arXiv preprint arXiv:2006.14042*, 2020.
- [30] Ambar Pal and René Vidal. A game theoretic analysis of additive adversarial attacks and defenses. *Advances in Neural Information Processing Systems*, 33:1345–1355, 2020.
- [31] Ludwig Schmidt, Shibani Santurkar, Dimitris Tsipras, Kunal Talwar, and Aleksander Madry. Adversarially robust generalization requires more data. *Advances in neural information processing systems*, 31, 2018.
- [32] Aditi Raghunathan, Sang Michael Xie, Fanny Yang, John C Duchi, and Percy Liang. Adversarial training can hurt generalization. *arXiv preprint arXiv:1906.06032*, 2019.
- [33] Leslie Rice, Eric Wong, and Zico Kolter. Overfitting in adversarially robust deep learning. In *International Conference on Machine Learning*, pages 8093–8104. PMLR, 2020.
- [34] Dongxian Wu, Shu-Tao Xia, and Yisen Wang. Adversarial weight perturbation helps robust generalization. *Advances in Neural Information Processing Systems*, 33:2958–2969, 2020.
- [35] Dong Yin, Ramchandran Kannan, and Peter Bartlett. Rademacher complexity for adversarially robust generalization. In *International conference on machine learning*, pages 7085–7094. PMLR, 2019.
- [36] Pranjal Awasthi, Natalie Frank, and Mehryar Mohri. Adversarial learning guarantees for linear hypotheses and neural networks. In *International Conference on Machine Learning*, pages 431–441. PMLR, 2020.
- [37] Farzan Farnia, Jesse M Zhang, and David Tse. Generalizable adversarial training via spectral normalization. *arXiv preprint arXiv:1811.07457*, 2018.
- [38] Idan Attias, Aryeh Kontorovich, and Yishay Mansour. Improved generalization bounds for robust learning. In *Algorithmic Learning Theory*, pages 162–183. PMLR, 2019.
- [39] Aleksander Madry, Aleksandar Makelov, Ludwig Schmidt, Dimitris Tsipras, and Adrian Vladu. Towards deep learning models resistant to adversarial attacks. *arXiv preprint arXiv:1706.06083*, 2017.
- [40] Yuichi Yoshida and Takeru Miyato. Spectral norm regularization for improving the generalizability of deep learning. *arXiv preprint arXiv:1705.10941*, 2017.
- [41] Takeru Miyato, Toshiki Kataoka, Masanori Koyama, and Yuichi Yoshida. Spectral normalization for generative adversarial networks. *arXiv preprint arXiv:1802.05957*, 2018.
- [42] Yuan Yao, Lorenzo Rosasco, and Andrea Caponnetto. On early stopping in gradient descent learning. *Constructive Approximation*, 26(2):289–315, 2007.
- [43] Ian J. Goodfellow, Jonathon Shlens, and Christian Szegedy. Explaining and harnessing adversarial examples. In Yoshua Bengio and Yann LeCun, editors, *3rd International Conference on Learning Representations, ICLR 2015, San Diego, CA, USA, May 7-9, 2015, Conference Track Proceedings*, 2015.

- [44] Diederik P Kingma and Jimmy Ba. Adam: A method for stochastic optimization. *arXiv preprint arXiv:1412.6980*, 2014.
- [45] Adam Paszke, Sam Gross, Francisco Massa, Adam Lerer, James Bradbury, Gregory Chanan, Trevor Killeen, Zeming Lin, Natalia Gimelshein, Luca Antiga, Alban Desmaison, Andreas Köpf, Edward Z. Yang, Zachary DeVito, Martin Raison, Alykhan Tejani, Sasank Chilamkurthy, Benoit Steiner, Lu Fang, Junjie Bai, and Soumith Chintala. Pytorch: An imperative style, high-performance deep learning library. In Hanna M. Wallach, Hugo Larochelle, Alina Beygelzimer, Florence d’Alché-Buc, Emily B. Fox, and Roman Garnett, editors, *Advances in Neural Information Processing Systems 32: Annual Conference on Neural Information Processing Systems 2019, NeurIPS 2019, December 8-14, 2019, Vancouver, BC, Canada*, pages 8024–8035, 2019.
- [46] Alex Krizhevsky, Geoffrey Hinton, et al. Learning multiple layers of features from tiny images. 2009.
- [47] Y Netzer, T. Wang, A. Coates, A. Bissacco, and A. Y. Ng. Reading digits in natural images with unsupervised feature learning. 2011.
- [48] Alex Krizhevsky, Ilya Sutskever, and Geoffrey E. Hinton. Imagenet classification with deep convolutional neural networks. In Peter L. Bartlett, Fernando C. N. Pereira, Christopher J. C. Burges, Léon Bottou, and Kilian Q. Weinberger, editors, *Advances in Neural Information Processing Systems 25: 26th Annual Conference on Neural Information Processing Systems 2012. Proceedings of a meeting held December 3-6, 2012, Lake Tahoe, Nevada, United States*, pages 1106–1114, 2012.
- [49] Christian Szegedy, Wei Liu, Yangqing Jia, Pierre Sermanet, Scott E. Reed, Dragomir Anguelov, Dumitru Erhan, Vincent Vanhoucke, and Andrew Rabinovich. Going deeper with convolutions. In *IEEE Conference on Computer Vision and Pattern Recognition, CVPR 2015, Boston, MA, USA, June 7-12, 2015*, pages 1–9. IEEE Computer Society, 2015.
- [50] Karen Simonyan and Andrew Zisserman. Very deep convolutional networks for large-scale image recognition. In Yoshua Bengio and Yann LeCun, editors, *3rd International Conference on Learning Representations, ICLR 2015, San Diego, CA, USA, May 7-9, 2015, Conference Track Proceedings*, 2015.
- [51] Kaiming He, Xiangyu Zhang, Shaoqing Ren, and Jian Sun. Deep residual learning for image recognition. In *2016 IEEE Conference on Computer Vision and Pattern Recognition, CVPR 2016, Las Vegas, NV, USA, June 27-30, 2016*, pages 770–778. IEEE Computer Society, 2016.
- [52] Peter L Bartlett and Shahar Mendelson. Rademacher and gaussian complexities: Risk bounds and structural results. *Journal of Machine Learning Research*, 3(Nov):463–482, 2002.

## Appendix A Proofs

### A.1 Proof of Proposition 1

To prove the proposition, note that the optimization problem for  $\lambda$ -optimal adversarial attack scheme can be written as

$$\max_{\delta: \mathcal{X} \times \mathcal{Y} \rightarrow \mathbb{R}^d} \mathbb{E} \left[ \ell(h_{\mathbf{w}}(\mathbf{X} + \delta(\mathbf{X}, Y)), Y) - \frac{\lambda}{2} \|\delta(\mathbf{X}, Y)\|^2 \right].$$

We observe that the above optimization problem decouples into separate problems for every  $(\mathbf{x}, y)$ , and hence  $\delta^*(\mathbf{x}, y)$  is the optimal solution to the following optimization problem

$$\max_{\delta \in \mathbb{R}^d} \ell(h_{\mathbf{w}}(\mathbf{x} + \delta), y) - \frac{\lambda}{2} \|\delta\|^2.$$

Since  $\ell \circ h_{\mathbf{w}}$  is assumed to be  $\lambda$ -smooth in  $\mathbf{x}$ , the objective function in the above optimization problem is a concave function of  $\delta$ . This is because the Hessian of the above objective function will be negative semi-definite as

$$\nabla_{\delta}^2 \left[ \ell(h_{\mathbf{w}}(\mathbf{x} + \delta), y) - \frac{\lambda}{2} \|\delta\|^2 \right] = \nabla_{\delta}^2 \ell(h_{\mathbf{w}}(\mathbf{x} + \delta), y) - \lambda I_{d \times d} \preceq \mathbf{0}. \quad (15)$$

Therefore, applying the first-order necessary condition implies that a globally optimal solution  $\delta^*(\mathbf{x}, y)$  to the above concave objective function will be the solution to

$$\nabla_{\mathbf{x}} \ell(h_{\mathbf{w}}(\mathbf{x} + \delta^*(\mathbf{x}, y)), y) - \lambda \delta^*(\mathbf{x}, y) = \mathbf{0}.$$

The above necessary and sufficient condition for  $\delta^*(\mathbf{x}, y)$  can be rewritten as:

$$(\mathbf{x} + \delta^*(\mathbf{x}, y)) - \frac{1}{\lambda} \nabla_{\mathbf{x}} \ell(h_{\mathbf{w}}(\mathbf{x} + \delta^*(\mathbf{x}, y)), y) = \mathbf{x}.$$

Note that this condition is equivalent to the following equation which completes the proof:

$$\delta^*(\mathbf{x}, y) = \left( \text{Id}_{\mathbf{x}} - \frac{1}{\lambda} \nabla_{\mathbf{x}} \ell \circ h_{\mathbf{w}} \right)^{-1} (\mathbf{x}) - \mathbf{x}.$$

## A.2 Proof of Theorem 1

To show Theorem 1, we first present the following lemmas.

**Lemma 1** ([37], Lemma 7). *Under Assumptions 1, 2, the substitute neural network's loss function  $\ell(h_{\mathbf{w}}(\mathbf{x}), y)$  is  $\kappa$ -smooth in input vector  $\mathbf{x}$ , i.e its gradient with respect to  $\mathbf{x}$  is  $\kappa$ -Lipschitz and satisfies*

$$\forall \mathbf{x}, \mathbf{x}' \in \mathcal{X}, y \in \mathcal{Y} : \quad \|\nabla_{\mathbf{x}} \ell(h_{\mathbf{w}}(\mathbf{x}), y) - \nabla_{\mathbf{x}} \ell(h_{\mathbf{w}}(\mathbf{x}'), y)\| \leq \kappa \|\mathbf{x} - \mathbf{x}'\|,$$

where  $\kappa = \left( \sum_{i=0}^L \prod_{j=0}^i \gamma_j \|W_j\| \right) \left( \prod_{i=0}^L \gamma_i \|W_i\| \right)$ .

**Lemma 2.** *Under Theorem 1's assumptions, the  $\lambda$ -optimal attack scheme  $\delta_{\mathbf{w}}^* : \mathcal{X} \times \mathcal{Y} \rightarrow \mathbb{R}^d$  satisfies the following output norm constraint for every  $(\mathbf{x}, y) \in \mathcal{X} \times \mathcal{Y}$ :*

$$\|\delta_{\mathbf{w}}^*(\mathbf{x}, y)\| \leq \frac{\prod_{i=0}^L \gamma_i \|W_i\|_2}{\lambda} = \frac{L_{\mathbf{w}}}{\lambda}.$$

*Proof.* Note that since  $\lambda > \left( \sum_{i=0}^L \prod_{j=0}^i \gamma_j \|W_j\| \right) \prod_{i=0}^L \gamma_i \|W_i\|_2$  holds according to Theorem 1's assumptions, the smoothness condition of Proposition 1 will hold according to Lemma 1. As a result, we have

$$\delta_{\mathbf{w}}^*(\mathbf{x}, y) = \frac{1}{\lambda} \nabla_{\mathbf{x}} \ell(h_{\mathbf{w}}(\mathbf{x} + \delta_{\mathbf{w}}^*(\mathbf{x}, y)), y).$$

Therefore,

$$\|\delta_{\mathbf{w}}^*(\mathbf{x}, y)\| \leq \frac{\|\nabla_{\mathbf{x}} \ell(h_{\mathbf{w}}(\mathbf{x} + \delta_{\mathbf{w}}^*(\mathbf{x}, y)), y)\|}{\lambda} \leq \frac{\prod_{i=0}^L \gamma_i \|W_i\|_2}{\lambda}.$$

The final inequality follows from the Lipschitz coefficient of DNN function  $h_{\mathbf{w}}$  which is the composition of linear transformation  $W_i$ 's (with Lipschitz constant  $\|W_i\|_2$ ) and activation non-linearity  $\phi_i$ 's (with Lipschitz constant  $\gamma_i$ ). Therefore, the proof is complete.  $\square$

**Lemma 3.** *Under Assumption 2, the substitute neural network  $h_{\mathbf{w}}$ 's gradient satisfies the following error bound under a perturbation matrix  $\Delta_k$  with  $L_2$ -operator norm  $\|\Delta_k\|_2 \leq t$  to wight matrix  $W_k$ , where we define  $\tilde{\mathbf{w}} = \text{vec}(W_0, \dots, W_{k-1}, W_k + \Delta_k, W_{k+1}, \dots, W_L)$ :*

$$\|\nabla_{\mathbf{x}} h_{\mathbf{w}}(\mathbf{x}) - \nabla_{\mathbf{x}} h_{\tilde{\mathbf{w}}}(\mathbf{x})\| \leq \frac{L_{\mathbf{w}} \sum_{i=k}^L \prod_{j=0}^i \gamma_j \|W_j\|}{\|W_k\|_2} \|\Delta_k\|_2$$

*Proof.* Note that the neural network's Jacobian with respect to the input follows from:

$$\mathbf{J}_{h_{\mathbf{w}}}(\mathbf{x}) = \prod_{i=0}^L W_i^\top \text{diag}(\phi'_i(h_{\mathbf{w}_{0:i}}(\mathbf{x}))).$$

In the above,  $h_{\mathbf{w}_{0:i}}(\mathbf{x})$  denotes the neural net's output at layer  $i$ . Therefore, for  $\tilde{\mathbf{w}}$  which is different from  $\mathbf{w}$  only at layer  $k$  we will have:

$$\begin{aligned} \|\mathbf{J}_{h_{\mathbf{w}}}(\mathbf{x}) - \mathbf{J}_{h_{\tilde{\mathbf{w}}}}(\mathbf{x})\|_2 &\leq \sum_{i=k}^L \left[ \left( \prod_{j=0}^L \gamma_j \|W_j\|_2 \right) \left( \prod_{j=0}^i \gamma_j \|W_j\|_2 \right) \right] \frac{\|\Delta_k\|_2}{\|W_k\|_2} \\ &= \left( \prod_{j=0}^L \gamma_j \|W_j\|_2 \right) \sum_{i=k}^L \left[ \prod_{j=0}^i \gamma_j \|W_j\|_2 \right] \frac{\|\Delta_k\|_2}{\|W_k\|_2} \\ &= \frac{L_{\mathbf{w}} \sum_{i=k}^L \prod_{j=0}^i \gamma_j \|W_j\|_2}{\|W_k\|_2} \|\Delta_k\|_2. \end{aligned}$$

The proof is hence finished.  $\square$

**Lemma 4.** Under Theorem 1's assumptions, the  $\lambda$ -optimal attack scheme  $\delta_{\mathbf{w}}^* : \mathcal{X} \times \mathcal{Y} \rightarrow \mathbb{R}^d$  satisfies the following error bound under a norm-bounded perturbation  $\Delta_k : \|\Delta_k\|_2 \leq t$ : to wight matrix  $W_k$  where we define  $\tilde{\mathbf{w}} = \text{vec}(W_0, \dots, W_{k-1}, W_k + \Delta_j, W_{k+1}, \dots, W_L)$ :

$$\|\delta_{\mathbf{w}}^*(\mathbf{x}, y) - \delta_{\tilde{\mathbf{w}}}^*(\mathbf{x}, y)\| \leq \frac{L_{\mathbf{w}} \sum_{i=k}^L \prod_{j=0}^i \gamma_j \|W_j\|_2}{\tau \lambda \|W_k\|_2} \|\Delta_k\|_2$$

*Proof.* Since  $\lambda > \left( \sum_{i=0}^L \prod_{j=0}^i \gamma_j \|W_j\|_2 \right) \prod_{i=0}^L \gamma_i \|W_i\|_2$  follows from Theorem 1's assumption, Proposition 1 will hold according to Lemma 1 and implies that

$$\delta_{\mathbf{w}}^*(\mathbf{x}, y) = \frac{1}{\lambda} \nabla_{\mathbf{x}} \ell(h_{\mathbf{w}}(\mathbf{x} + \delta_{\mathbf{w}}^*(\mathbf{x}, y)), y).$$

As a result,

$$\begin{aligned} &\|\delta_{\mathbf{w}}^*(\mathbf{x}, y) - \delta_{\tilde{\mathbf{w}}}^*(\mathbf{x}, y)\| \\ &= \frac{1}{\lambda} \left\| \nabla_{\mathbf{x}} \ell(h_{\mathbf{w}}(\mathbf{x} + \delta_{\mathbf{w}}^*(\mathbf{x}, y)), y) - \nabla_{\mathbf{x}} \ell(h_{\tilde{\mathbf{w}}}(\mathbf{x} + \delta_{\tilde{\mathbf{w}}}^*(\mathbf{x}, y)), y) \right\| \\ &\leq \frac{1}{\lambda} \left\| \nabla_{\mathbf{x}} \ell(h_{\mathbf{w}}(\mathbf{x} + \delta_{\mathbf{w}}^*(\mathbf{x}, y)), y) - \nabla_{\mathbf{x}} \ell(h_{\mathbf{w}}(\mathbf{x} + \delta_{\tilde{\mathbf{w}}}^*(\mathbf{x}, y)), y) \right\| \\ &\quad + \frac{1}{\lambda} \left\| \nabla_{\mathbf{x}} \ell(h_{\mathbf{w}}(\mathbf{x} + \delta_{\tilde{\mathbf{w}}}^*(\mathbf{x}, y)), y) - \nabla_{\mathbf{x}} \ell(h_{\tilde{\mathbf{w}}}(\mathbf{x} + \delta_{\tilde{\mathbf{w}}}^*(\mathbf{x}, y)), y) \right\| \\ &\stackrel{(a)}{\leq} \frac{\text{Lip}(\nabla_{\mathbf{x}} \ell \circ h_{\mathbf{w}})}{\lambda} \|\delta_{\mathbf{w}}^*(\mathbf{x}, y) - \delta_{\tilde{\mathbf{w}}}^*(\mathbf{x}, y)\| + \frac{L_{\mathbf{w}} \sum_{i=k}^L \prod_{j=0}^i \gamma_j \|W_j\|_2}{\lambda \|W_k\|_2} \|\Delta_k\|_2 \\ &\stackrel{(b)}{\leq} \frac{L_{\mathbf{w}} \sum_{i=k}^L \prod_{j=0}^i \gamma_j \|W_j\|_2}{\lambda} \|\delta_{\mathbf{w}}^*(\mathbf{x}, y) - \delta_{\tilde{\mathbf{w}}}^*(\mathbf{x}, y)\| + \frac{L_{\mathbf{w}} \sum_{i=0}^L \prod_{j=0}^i \gamma_j \|W_j\|_2}{\lambda \|W_k\|_2} \|\Delta_k\|_2 \\ &\stackrel{(c)}{\leq} (1 - \tau) \|\delta_{\mathbf{w}}^*(\mathbf{x}, y) - \delta_{\tilde{\mathbf{w}}}^*(\mathbf{x}, y)\| + \frac{L_{\mathbf{w}} \sum_{i=k}^L \prod_{j=0}^i \gamma_j \|W_j\|_2}{\lambda \|W_k\|_2} \|\Delta_k\|_2 \end{aligned}$$

Here, (a) follows from the definition of Lipschitz constant and Lemma 3's weight perturbation bound. (b) comes from a direct application of Lemma 1, and (c) follows from Theorem 1' assumption. Therefore, the



above inequalities collectively lead to the following bound, which completes the proof:

$$\tau \|\delta_{\mathbf{w}}^*(\mathbf{x}, y) - \delta_{\tilde{\mathbf{w}}}^*(\mathbf{x}, y)\| \leq \frac{L_{\mathbf{w}} \sum_{i=k}^L \prod_{j=0}^i \gamma_j \|W_j\|}{\lambda \|W_k\|_2} \|\Delta_k\|_2.$$

□

To prove Theorem 1, we follow a covering-number-based approach similar to the generalization analysis in [16] for the standard non-adversarial deep supervised learning problem. To do this, we consider the norm constraints  $\|W_i\|_2 \leq a'_i$ ,  $\|W_i\|_{2,1} \leq b'_i$  for every  $i = 0, \dots, L$ , and  $\|V_j\|_2 \leq a_i$ ,  $\|V_j\|_{2,1} \leq b_i$  for every  $j = 0, \dots, K$ . Now, we define the following covering resolution parameters for the classifier and substitute DNNs' different layers:

$$\epsilon'_k = \frac{\tau \lambda a'_k \alpha'_k \epsilon}{2 \left( \prod_{i=0}^K \xi_i a_i \right) \left( \prod_{i=0}^L \gamma_i a'_i \right) \left( \sum_{i=k}^L \prod_{j=0}^i \gamma_j a'_j \right)}, \text{ where } \alpha'_k = \frac{1}{A'} \frac{b'_k{}^{2/3}}{a'_k{}^{2/3}}, \quad A' = \sum_{i=0}^L \frac{b'_i{}^{2/3}}{a'_i{}^{2/3}}$$

$$\epsilon_j = \frac{a_j \alpha_j \epsilon}{2 \prod_{i=j}^K \gamma_i a_i}, \text{ where } \alpha_j = \frac{1}{A} \frac{b_j{}^{2/3}}{a_j{}^{2/3}}, \quad A = \sum_{i=0}^K \frac{b_i{}^{2/3}}{a_i{}^{2/3}}.$$

Note that Lemma 4 implies that by finding an  $\epsilon'_k$ -covering for each  $W_k$  and  $\epsilon_j$ -covering for each  $V_j$ , the covering resolution for  $\mathcal{F} \circ \Delta_H|_S$  will be upper-bounded by

$$\sum_{k=0}^L \left[ \frac{L_{\mathbf{w}} L_{\mathbf{v}} \sum_{i=k}^L \prod_{j=0}^i \gamma_j \|W_j\|}{\tau \lambda \|W_k\|_2} \epsilon'_k \right] + \sum_{k=0}^K \left[ \frac{\prod_{i=k}^K \gamma_i \|V_i\|_2}{\|V_k\|_2} \epsilon_k \right] = \epsilon.$$

Therefore, by applying Lemma A.7 from [16] we will have the following bound on the  $\epsilon$ -covering-number for the set  $\mathcal{F} \circ \Delta_H|_S = \{\ell(f_{\mathbf{v}}(\mathbf{X} + \delta_{\mathbf{w}}^*(\mathbf{X}, Y))) : \forall 0 \leq i \leq K : \|V_i\|_2 \leq a_i, \|V_i\|_{2,1} \leq b_i, \forall 0 \leq j \leq L : \|W_j\|_2 \leq a'_j, \|W_j\|_{2,1} \leq b'_j\}$

$$\begin{aligned} & \log \mathcal{N}(\mathcal{F} \circ \Delta_H|_S, \|\cdot\|_2, \epsilon) \\ & \leq \sum_{i=0}^L \sup_{\mathbf{w}_{-i}, \mathbf{v} \in \mathcal{W}, \mathcal{V}} \left[ \log \mathcal{N}(\{\delta_{\mathbf{w}}^*(\mathbf{X}, Y) : \|\mathbf{W}_i\|_2 \leq a'_i, \|\mathbf{W}_i\|_{2,1} \leq b'_i\}, \|\cdot\|_2, \epsilon'_i) \right] \\ & \quad + \sum_{i=0}^K \sup_{\mathbf{w}, \mathbf{v}_{-i} \in \mathcal{W}, \mathcal{V}} \left[ \log \mathcal{N}(\{h_{\mathbf{v}_{0:i}}(\mathbf{X}), Y) : \|\mathbf{V}_i\|_2 \leq a_i, \|\mathbf{V}_i\|_{2,1} \leq b_i\}, \|\cdot\|_2, \epsilon_i) \right] \\ & \leq \sum_{i=0}^L \sup_{\mathbf{w}_{-i}, \mathbf{v} \in \mathcal{W}, \mathcal{V}} \left[ \log \mathcal{N}(\{\delta_{\mathbf{w}}^*(\mathbf{X}, Y) : \|\mathbf{W}_i\|_{2,1} \leq b'_i\}, \|\cdot\|_2, \epsilon'_i) \right] \\ & \quad + \sum_{i=0}^K \sup_{\mathbf{w}, \mathbf{v}_{-i} \in \mathcal{W}, \mathcal{V}} \left[ \log \mathcal{N}(\{h_{\mathbf{v}_{0:i}}(\mathbf{X}), Y) : \|\mathbf{V}_i\|_{2,1} \leq b_i\}, \|\cdot\|_2, \epsilon_i) \right] \\ & \leq \sum_{i=0}^L \left[ \sup_{\mathbf{w}_{-i}, \mathbf{v} \in \mathcal{W}, \mathcal{V}} \frac{b'_i{}^2 \|\delta_{\mathbf{w}}^*(\mathbf{X}, Y)\|_2^2}{\epsilon_i'^2} \log(2W^2) \right] \\ & \quad + \sum_{i=0}^K \left[ \sup_{\mathbf{w}, \mathbf{v}_{-i} \in \mathcal{W}, \mathcal{V}} \frac{b_i^2 \|h_{\mathbf{v}_{0:i}}(\mathbf{X})\|_2^2}{\epsilon_i^2} \log(2W^2) \right] \\ & \leq \sum_{i=0}^K \left[ \sup_{\mathbf{w}_{-i}, \mathbf{v} \in \mathcal{W}, \mathcal{V}} \frac{L_{\mathbf{w}}^2 \log(2W^2) b_i'^2}{\lambda^2 \epsilon^2 \epsilon_i'^2} \right] \end{aligned}$$

$$\begin{aligned}
& + \sum_{i=0}^L \left[ \frac{4b_i^2 (B + \frac{\prod_{i=0}^L \gamma_i a'_i}{\lambda})^2 \prod_{i=0}^K \xi_i^2 a_i^2 \sum_{i=0}^K \frac{b_i^2}{\alpha_i^2 a_i^2}}{\epsilon^2} \right] \\
\leq & \frac{\log(2W^2) \prod_{i=0}^L \gamma_i^2 a_i'^2}{\lambda^2 \epsilon^2} \sum_{k=0}^K \left[ \frac{b_i'^2 (\sum_{i=k}^L \prod_{j=0}^i \gamma_i a_i)^2}{\alpha_i'^2 a_i'^2} \right] \\
& + \sum_{i=0}^L \left[ \frac{4b_i^2 (B + \frac{\prod_{i=0}^L \gamma_i a'_i}{\lambda})^2 \prod_{i=0}^K \xi_i^2 a_i^2 \sum_{i=0}^K \frac{b_i^2}{\alpha_i^2 a_i^2}}{\epsilon^2} \right] \\
\leq & \frac{\log(2W^2) \prod_{i=0}^L \gamma_i^2 a_i'^2 (\sum_{i=0}^L \prod_{j=0}^i \gamma_i a_i)^2}{\lambda^2 \epsilon^2} \sum_{k=0}^K \left[ \frac{b_k'^2}{\alpha_k'^2 a_k'^2} \right] \\
& + \sum_{i=0}^L \left[ \frac{4b_i^2 (B + \frac{\prod_{i=0}^L \gamma_i a'_i}{\lambda})^2 \prod_{j=0}^K \xi_j^2 a_j^2 \sum_{k=0}^K \frac{b_k^2}{\alpha_k^2 a_k^2}}{\epsilon^2} \right] \\
\leq & \frac{4 \log(2W^2) \prod_{i=0}^L \gamma_i^2 a_i'^2 (\sum_{i=0}^L \prod_{j=0}^i \gamma_j a_j)^2}{\lambda^2 \epsilon^2} \sum_{i=0}^L \left[ \frac{b_i'^2}{\alpha_i'^2 a_i'^2} \right] \\
& + \frac{4 \log(2W^2) (B + \frac{\prod_{i=0}^L \gamma_i a'_i}{\lambda})^2 \prod_{i=0}^K \xi_i^2 a_i^2}{\epsilon^2} \sum_{i=0}^K \left[ \frac{b_i^2}{\alpha_i^2 a_i^2} \right] \\
= & \frac{C}{\epsilon^2}
\end{aligned}$$

where we define

$$\begin{aligned}
C := & 4 \log(2W^2) \left[ \frac{\prod_{i=0}^L \gamma_i^2 a_i'^2 (\sum_{i=0}^L \prod_{j=0}^i \gamma_j a_j)^2}{\lambda^2} \left[ \sum_{i=0}^L \frac{b_i'^{2/3}}{\alpha_i'^{2/3}} \right]^3 \right. \\
& \left. + (B + \frac{\prod_{i=0}^L \gamma_i a'_i}{\lambda})^2 \prod_{i=0}^K \xi_i^2 a_i^2 \left[ \sum_{i=0}^K \frac{b_i^{2/3}}{\alpha_i^{2/3}} \right]^3 \right].
\end{aligned}$$

Now, based on the above covering-number bound, we use the Dudley entropy integral bound [16] which bounds the empirical Rademacher complexity of  $\mathcal{F} \circ \Delta_{\mathcal{H}}|_S$  as

$$\begin{aligned}
\mathcal{R}(\mathcal{F} \circ \Delta_{\mathcal{H}}|_S) & \leq \inf_{\alpha \geq 0} \left\{ \frac{4\alpha}{\sqrt{n}} + \frac{12}{n} \int_{\alpha}^{\sqrt{n}} \sqrt{\log \mathcal{N}(\mathcal{F} \circ \Delta_{\mathcal{H}}|_S, \|\cdot\|_2, \epsilon)} d\epsilon \right\} \\
& \leq \inf_{\alpha \geq 0} \left\{ \frac{4\alpha}{\sqrt{n}} + \log\left(\frac{\sqrt{n} 12\sqrt{C}}{\alpha n}\right) \right\} \\
& \leq \frac{4}{n^{3/2}} + \frac{18 \log(n) \sqrt{C}}{n}
\end{aligned}$$

where the last line follows from choosing  $\alpha = 1/n$ . Also, note that since for every non-negative constants  $a, b \geq 0$  we have  $\sqrt{a+b} \leq \sqrt{a} + \sqrt{b}$ , then

$$\begin{aligned}
\sqrt{C} & \leq 2\sqrt{\log(2D^2)} \left[ \frac{\prod_{i=0}^L \gamma_i a_i' (\sum_{i=0}^L \prod_{j=0}^i \gamma_j a_j)}{\lambda} \left[ \sum_{i=0}^L \frac{b_i'^{2/3}}{\alpha_i'^{2/3}} \right]^{3/2} \right. \\
& \quad \left. + (B + \frac{\prod_{i=0}^L \gamma_i a'_i}{\lambda}) \prod_{i=0}^K \xi_i a_i \left[ \sum_{i=0}^K \frac{b_i^{2/3}}{\alpha_i^{2/3}} \right]^{3/2} \right].
\end{aligned}$$

Consequently, we have the following bound where  $R_{\mathcal{V}}$  and  $R_{\mathcal{W}}$  are defined as in Theorem 1:

$$\mathcal{R}(\mathcal{F} \circ \Delta_{\mathcal{H}}|_S) \leq \mathcal{O}\left(\frac{(B + \frac{L_{\mathbf{w}}}{\lambda})(R_{\mathcal{V}} + \frac{1}{\tau^2}L_{\mathbf{w}}R_{\mathcal{W}}) \log(n)}{n} \log(D)\right)$$

Therefore, according to standard Rademacher complexity-based generalization bounds [52], for every  $\omega > 0$  with probability at least  $1 - \omega$  we have for every  $\mathbf{v}, \mathbf{w} \in \mathcal{V}, \mathcal{W}$ :

$$\begin{aligned} & \frac{1}{n} \sum_{i=1}^n \left[ \ell(f_{\mathbf{v}}(\mathbf{x}_i + \delta_{\mathbf{w}}^*(\mathbf{x}_i, y_i)), y_i) \right] - \mathbb{E} \left[ \ell(f_{\mathbf{v}}(\mathbf{X} + \delta_{\mathbf{w}}^*(\mathbf{X}, Y)), Y) \right] \\ & \leq \mathcal{O}\left(c\sqrt{\frac{\log(1/\omega)}{n}} + \frac{(B + \frac{L_{\mathbf{w}}}{\lambda})(R_{\mathcal{V}} + \frac{1}{\tau^2}L_{\mathbf{w}}R_{\mathcal{W}}) \log(n)}{n} \log(D)\right), \end{aligned}$$

which implies that

$$\begin{aligned} \epsilon_{\text{gen}}(\delta_{\mathbf{w}}^*) &= \min_{\mathbf{v} \in \mathcal{V}} \left\{ \frac{1}{n} \sum_{i=1}^n \left[ \ell(f_{\mathbf{v}}(\mathbf{x}_i + \delta_{\mathbf{w}}^*(\mathbf{x}_i, y_i)), y_i) \right] \right\} - \min_{\mathbf{v} \in \mathcal{V}} \left\{ \mathbb{E} \left[ \ell(f_{\mathbf{v}}(\mathbf{X} + \delta_{\mathbf{w}}^*(\mathbf{X}, Y)), Y) \right] \right\} \\ &\leq \max_{\mathbf{v} \in \mathcal{V}} \left\{ \frac{1}{n} \sum_{i=1}^n \left[ \ell(f_{\mathbf{v}}(\mathbf{x}_i + \delta_{\mathbf{w}}^*(\mathbf{x}_i, y_i)), y_i) \right] - \mathbb{E} \left[ \ell(f_{\mathbf{v}}(\mathbf{X} + \delta_{\mathbf{w}}^*(\mathbf{X}, Y)), Y) \right] \right\} \\ &\leq \mathcal{O}\left(c\sqrt{\frac{\log(1/\omega)}{n}} + \frac{(B + \frac{L_{\mathbf{w}}}{\lambda})(R_{\mathcal{V}} + \frac{1}{\tau^2}L_{\mathbf{w}}R_{\mathcal{W}}) \log(n)}{n} \log(D)\right). \end{aligned}$$

Therefore, the theorem's proof is complete.

## Appendix B Additional Numerical Experiments

In this section, we report the complete set of our numerical results. Table 3 shows the complete results for DNNs regularized by early stopping, i.e. the complete version of Table 2. Moreover, Tables 5,6,7 are the full versions of Table 1, demonstrating the relationship between generalization errors and transferability rates of the discussed datasets and DNN architectures. In addition to our earlier results, the accuracies for adversarially-perturbed training and test samples are also included in the tables.

In addition to the previous results, we also present the transferability rates averaged over test samples whose adversarial examples are predicted correctly by both the regularized and unregularized substitute DNNs. The transferability rates over those test samples intersecting the correctly predicted samples by regularized and unregularized substitute DNNs are shown in Tables 3,5,6, and 7 under the title Transferability Rate-Int. Our numerical results suggest that over the test samples correctly predicted by both regularized and unregularized DNNs, a better generalization score again results in higher transferability rates for designed adversarial examples.

Table 3: Generalization and transferability rates for different DNN architectures and image datasets with and without early stopping (ES)

Dataset	Model	Method	Train Acc	Test Acc	Gen.Err.	Transferability Rate(VGG16)	Transferability Rate(ResNet18)
Cifar10	Inception	PGM	0.970	0.453	0.517	0.127	0.104
		PGM-ES	0.591	0.518	0.073	0.198	0.172
		FGM	0.997	0.529	0.467	0.100	0.089
		FGM-ES	0.657	0.530	0.126	0.170	0.147
	Alexnet	PGM	1.000	0.421	0.579	0.098	0.077
		PGM-ES	0.548	0.487	0.061	0.154	0.136
		FGM	1.000	0.480	0.520	0.100	0.087
		FGM-ES	0.594	0.501	0.092	0.152	0.127
Cifar100	Inception	PGM	0.877	0.231	0.646	0.283	0.258
		PGM-ES	0.408	0.271	0.137	0.330	0.286
		FGM	0.984	0.272	0.711	0.270	0.239
		FGM-ES	0.457	0.312	0.146	0.327	0.289
	Alexnet	PGM	0.966	0.202	0.764	0.252	0.227
		PGM-ES	0.338	0.248	0.091	0.294	0.266
		FGM	0.990	0.234	0.756	0.261	0.232
		FGM-ES	0.399	0.278	0.122	0.291	0.259
SVHN	Inception	PGM	0.925	0.585	0.341	0.207	0.220
		PGM-ES	0.711	0.654	0.057	0.298	0.322
		FGM	0.998	0.619	0.380	0.136	0.129
		FGM-ES	0.898	0.718	0.180	0.213	0.219
	Alexnet	PGM	0.848	0.541	0.307	0.211	0.228
		PGM-ES	0.624	0.594	0.030	0.256	0.278
		FGM	0.949	0.576	0.373	0.157	0.170
		FGM-ES	0.691	0.627	0.064	0.241	0.260

Table 4: Generalization and transferability rates for different DNN architectures and image datasets with and without early stopping (ES), Transferability Rate-Int. means averaged transferability rate on adversarial examples correctly labeled by both the regularized and unregularized DNNs.

Dataset	Model	Method	Gen.Err.	Transferability Rate-Int.(VGG16)	Transferability Rate-Int.(ResNet18)
Cifar10	Inception	PGM	0.517	0.030	0.127
		PGM-ES	0.073	0.063	0.198
		FGM	0.467	0.032	0.100
		FGM-ES	0.126	0.077	0.170
	Alexnet	PGM	0.579	0.037	0.098
		PGM-ES	0.061	0.077	0.154
		FGM	0.520	0.035	0.100
		FGM-ES	0.092	0.076	0.152
Cifar100	Inception	PGM	0.646	0.141	0.283
		PGM-ES	0.137	0.160	0.330
		FGM	0.711	0.126	0.270
		FGM-ES	0.146	0.154	0.327
	Alexnet	PGM	0.764	0.114	0.252
		PGM-ES	0.091	0.159	0.294
		FGM	0.756	0.127	0.261
		FGM-ES	0.122	0.180	0.291
SVHN	Inception	PGM	0.341	0.024	0.207
		PGM-ES	0.057	0.102	0.298
		FGM	0.380	0.010	0.136
		FGM-ES	0.180	0.103	0.213
	Alexnet	PGM	0.307	0.044	0.211
		PGM-ES	0.030	0.080	0.256
		FGM	0.373	0.013	0.157
		FGM-ES	0.064	0.092	0.241

Table 5: Generalization and transferability rates on CIFAR-10 data, with and without using spectral regularization

Dataset	Model	Method	$\beta$	Train Acc	Test Acc	Gen.Err.	Transferability Rate(VGG16)	Transferability Rate(ResNet18)		
Cifar10	Inception	FGM( $L_2$ )	$\infty$	0.998	0.532	0.466	0.092	0.078		
			1	0.830	0.511	0.320	0.136	0.113		
			1.3	0.936	0.479	0.456	0.124	0.097		
			1.6	0.997	0.509	0.488	0.099	0.084		
			2	0.999	0.541	0.458	0.087	0.073		
			3	1.000	0.554	0.445	0.090	0.077		
		PGM( $L_2$ )	$\infty$	0.951	0.443	0.508	0.104	0.084		
			1	0.759	0.502	0.258	0.150	0.134		
			1.3	0.913	0.459	0.454	0.125	0.099		
			1.6	0.945	0.447	0.499	0.115	0.095		
			2	0.979	0.451	0.529	0.110	0.092		
			3	0.988	0.468	0.520	0.103	0.082		
		FGM( $L_\infty$ )	$\infty$	0.946	0.442	0.504	0.124	0.101		
			1	0.694	0.451	0.243	0.191	0.153		
			1.3	0.842	0.421	0.421	0.165	0.129		
			1.6	0.951	0.419	0.531	0.129	0.106		
			2	0.980	0.453	0.527	0.121	0.103		
			3	0.988	0.470	0.517	0.112	0.091		
		PGM( $L_\infty$ )	$\infty$	0.708	0.525	0.184	0.419	0.393		
			1	0.627	0.545	0.082	0.497	0.474		
			1.3	0.674	0.534	0.140	0.466	0.443		
			1.6	0.710	0.520	0.190	0.442	0.422		
			2	0.739	0.505	0.234	0.408	0.389		
			3	0.745	0.504	0.241	0.398	0.380		
	Alexnet	FGM( $L_2$ )	$\infty$	1.000	0.495	0.505	0.089	0.070		
			1	0.977	0.526	0.451	0.147	0.122		
			1.3	1.000	0.496	0.504	0.132	0.105		
			1.6	1.000	0.474	0.526	0.115	0.090		
			2	1.000	0.477	0.523	0.108	0.088		
			3	1.000	0.496	0.504	0.098	0.079		
			PGM( $L_2$ )	$\infty$	0.999	0.454	0.545	0.105	0.087	
				1	0.861	0.519	0.342	0.162	0.139	
				FGM( $L_\infty$ )	$\infty$	0.996	0.400	0.596	0.102	0.089
					1	0.914	0.426	0.487	0.199	0.169
					1.3	0.998	0.387	0.610	0.169	0.142
					1.6	1.000	0.368	0.632	0.146	0.120
		2	1.000		0.420	0.580	0.128	0.106		
		3	1.000		0.435	0.565	0.115	0.096		
		PGM( $L_\infty$ )	$\infty$	0.685	0.474	0.211	0.446	0.423		
			1	0.628	0.473	0.156	0.472	0.457		
			1.3	0.680	0.436	0.245	0.441	0.423		
			1.6	0.697	0.420	0.277	0.421	0.403		
			2	0.679	0.408	0.271	0.404	0.388		
			3	0.628	0.439	0.189	0.426	0.405		

Table 6: Generalization and transferability rates on CIFAR-100 dataset, with and without spectral regularization.

Dataset	Model	Method	$\beta$	Train Acc	Test Acc	Gen.Err.	Transferability Rate(VGG16)	Transferability Rate(ResNet18)		
Cifar100	Inception	FGM( $L_2$ )	$\infty$	0.996	0.279	0.717	0.268	0.236		
			1	0.761	0.277	0.484	0.250	0.290		
			1.3	0.853	0.294	0.558	0.313	0.275		
			1.6	0.998	0.260	0.738	0.236	0.263		
			2	1.000	0.284	0.715	0.238	0.272		
			3	0.999	0.262	0.736	0.221	0.257		
			$\infty$	0.857	0.255	0.602	0.303	0.270		
		PGM( $L_2$ )	1	0.604	0.255	0.349	0.329	0.297		
			1.3	0.750	0.256	0.494	0.330	0.301		
			1.6	0.893	0.230	0.664	0.305	0.265		
			2	0.868	0.233	0.635	0.307	0.277		
			3	0.948	0.220	0.728	0.290	0.248		
			Alexnet	FGM( $L_2$ )	$\infty$	1.000	0.242	0.758	0.258	0.232
					1	0.925	0.315	0.611	0.342	0.310
	1.3	1.000			0.289	0.710	0.304	0.266		
	1.6	1.000			0.285	0.715	0.291	0.248		
	2	1.000			0.284	0.716	0.288	0.253		
	PGM( $L_2$ )	3		1.000	0.269	0.730	0.265	0.240		
		$\infty$		1.000	0.210	0.789	0.229	0.260		
		1		0.889	0.288	0.601	0.323	0.353		
		1.3		0.998	0.234	0.763	0.307	0.282		
		1.6		1.000	0.227	0.773	0.306	0.261		
	2	1.000	0.229	0.771	0.283	0.259				
	3	1.000	0.213	0.787	0.272	0.238				

Table 7: Generalization and transferability rates on SVHN dataset, with and without spectral regularization.

Dataset	Model	Method	$\beta$	Train Acc	Test Acc	Gen.Err.	Transferability Rate(VGG16)	Transferability Rate(ResNet18)
SVHN	Inception	FGM( $L_2$ )	$\infty$	0.991	0.618	0.373	0.134	0.126
			1	0.848	0.645	0.203	0.277	0.257
			1.3	0.967	0.605	0.362	0.223	0.209
			1.6	0.998	0.573	0.426	0.202	0.187
			2	1.000	0.571	0.429	0.158	0.149
			3	1.000	0.642	0.358	0.121	0.118
		PGM( $L_2$ )	$\infty$	0.708	0.524	0.184	0.393	0.419
			1	0.627	0.545	0.082	0.474	0.497
			1.3	0.674	0.534	0.140	0.466	0.443
			1.6	0.710	0.520	0.190	0.442	0.422
			2	0.739	0.505	0.234	0.408	0.389
			3	0.745	0.504	0.241	0.398	0.380
	Alexnet	FGM( $L_2$ )	$\infty$	0.991	0.618	0.373	0.134	0.126
			1	0.848	0.645	0.203	0.277	0.257
			1.3	0.967	0.605	0.362	0.223	0.209
			1.6	0.998	0.573	0.426	0.202	0.187
			2	1.000	0.571	0.429	0.158	0.149
			3	0.999	0.581	0.418	0.145	0.133
		PGM( $L_2$ )	$\infty$	0.844	0.546	0.298	0.211	0.225
			1	0.817	0.618	0.199	0.276	0.292
			1.3	0.936	0.570	0.366	0.229	0.244
			1.6	0.976	0.539	0.437	0.197	0.209
			2	0.992	0.520	0.473	0.172	0.182
			3	0.986	0.511	0.476	0.150	0.155



Table 8: Generalization and transferability rates for different DNN architectures and image datasets with and without spectral regularization. Transferability Rate-Int. means averaged transferability rate on adversarial examples correctly labeled by both the regularized and unregularized DNNs.

Dataset	Model	Method	$\beta$	Gen.Err.	Transferability Rate-Int(VGG16)	Transferability Rate-Int(ResNet18)
Cifar10	Inception	FGM( $L_2$ )	$\infty$	0.466	0.032	0.026
			1	0.320	0.077	0.058
		PGM( $L_2$ )	$\infty$	0.508	0.030	0.026
			1	0.258	0.063	0.052
		FGM( $L_\infty$ )	$\infty$	0.504	0.029	0.028
			1	0.243	0.070	0.090
	Alexnet	PGM( $L_\infty$ )	$\infty$	0.184	0.136	0.181
			1	0.082	0.182	0.162
		FGM( $L_2$ )	$\infty$	0.505	0.035	0.029
			1	0.451	0.076	0.068
		PGM( $L_2$ )	$\infty$	0.545	0.037	0.030
			1	0.342	0.077	0.063
Cifar100	Alexnet	FGM( $L_\infty$ )	$\infty$	0.596	0.039	0.019
			1	0.487	0.089	0.070
		PGM( $L_\infty$ )	$\infty$	0.211	0.227	0.222
			1	0.156	0.271	0.248
SVHN	Inception	FGM( $L_2$ )	$\infty$	0.717	0.126	0.112
			1.3	0.558	0.154	0.131
		PGM( $L_2$ )	$\infty$	0.602	0.141	0.123
			1.3	0.494	0.160	0.141
	Alexnet	FGM( $L_2$ )	$\infty$	0.758	0.127	0.101
			1	0.611	0.180	0.159
SVHN	Inception	PGM( $L_2$ )	$\infty$	0.789	0.114	0.108
			1	0.601	0.159	0.151
		FGM( $L_2$ )	$\infty$	0.373	0.010	0.013
			1	0.203	0.103	0.125
	Alexnet	PGM( $L_2$ )	$\infty$	0.342	0.024	0.031
			1	0.115	0.102	0.125
SVHN	Alexnet	FGM( $L_2$ )	$\infty$	0.373	0.013	0.014
			1	0.203	0.092	0.112
	PGM( $L_2$ )	$\infty$	0.298	0.044	0.053	
		1	0.199	0.080	0.101	